Muon Containment in the Near Detector

Emily Maher & Jeff Nelson
University of Minnesota

Abstract

We have studied muon containment in the near detector for all three beams, two different fiducial volumes, and for a crude representation of the low-energy beam-plug spectrum. For each of these scenarios we have studied the effects over the full range of currents allowed in the near detector coil. For all ND CC conditions we found that currents above 20kA-turns are acceptable. We also found the coil-stopping muons are not a significant issue for selecting the operating current. Therefore the mean-field specification is not strongly driven by fiducial CC muons. Field-matching requirements with respect to the FD (esp. for muon calibration) or containment requirements for non-fiducial CC muons may, however, define the specification. Future work should focus on these issues.

Introduction

Two issues drove the magnetic design of the near detector (ND): containment of muons in the H66 (three-horn, high-energy) beam and ability to fabricate 1" steel plate. The design lead to a high-current coil design delivering up to 40kA-turns. This study revisits muon containment in light of the low-energy baseline configuration with and eye towards reoptimization of the operating current for the near detector coil. Earlier work associated with ND design working group indicated a possible problem of over focussing LE muons at the full operating current. It was noted that muons often pass through the coil bore and exit the other side, however, there was also an apparent problem with many particles stopping inside the bore. These effects were investigated using the final ND module and bypass configurations.

Field Maps

Bob Wands has generated a series of eight ND field maps for current in 5kA steps from 5kA to 40kA. We also investigated the case of no magnetic field. All of these maps have been installed in the standard GMINOS / BMAP repository. They are map numbers 151 to 158. Map 158 (40kA) is the baseline ND configuration and should be used for all future ND studies. The modulus of the field is plotted in the following figure.

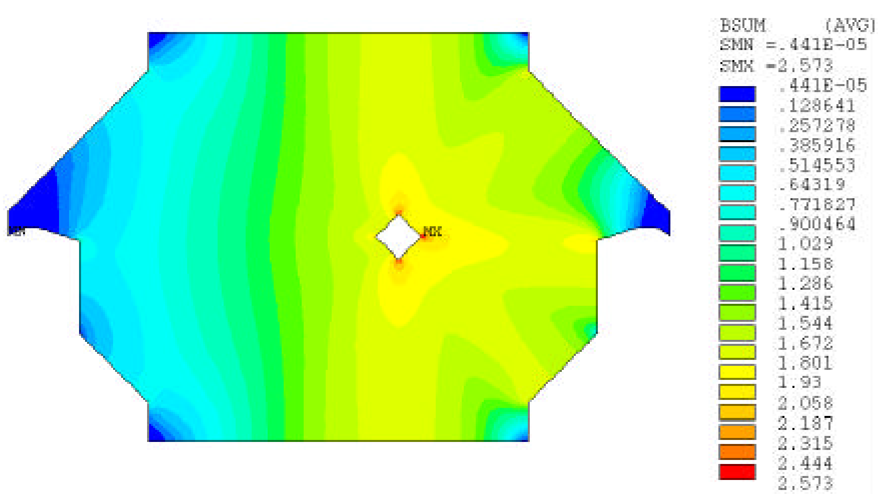

Data

Samples of ~800 events were generated for the three beams, nine different currents, and two different fiducial cuts (50cm and 25cm radii). We also generated samples events for each current in the LE beam with a 25cm fiducial cut and a cut on $E_{\nu,true} < 8$ GeV. This provides a crude understanding of containment in the presence of the beam-plug. It is also interesting since the near detector is long enough to range out muons up to 8GeV. Therefore any muons from these events that leave the side of the detector will have significantly degraded muon momentum resolution.

Analysis

For each dataset we investigated fiducial muon leakage out the sides of the detector. Due to the 58mrad angle of the beam, muons tend to fall out of the bottom of the near detector. We recorded leakage both from of the top and bottom of the near detector. Events leaving the back of the detector we not investigated.

Tracks ending within 2 strips of the edges of the detector were entered in the leakage total. On the return side of the detector some tracks can exit the instrumented area and returned to stop inside the instrumented volume. These tracks should have robust range measurements and are not considered "leakage" but did receive a separate tally.

Tracks that entered the coil and stopped with less than 2 hits on the "far" side of the hole were called "coil stoppers". Due to the uncertainties in the end point of the tracks they will be measured using magnetic curvature. Hence, there are considered a type of "leakage." The current ND geometry in GMINOS included scintillator coverage up to the coil collar in the fully instrumented planes. A custom LABRYNTH job was created to investigate these events in detail. The final ND coil bypass geometry (from Ingrid Fang) was included in the analysis code and all hits in the "bypass region" were deleted before analysis to understand the full impact of the dead volumes. A custom ROOT-based display was developed to aid in this analysis.

Results

The leakage tallies and rates for the various conditions are summarized in the following tables and plots. The tables for the truncated LE spectrum are shown first followed by the other cases.

I (kA)	Total # CC events	Top	Bottom	Coil
0	520	0	24	0
5	537	0	8	9
10	549	1	6	3
15	541	1	4	11
20	545	0	5	11
25	559	0	1	7
30	530	1	5	6
35	542	0	1	9
40	561	2	5	13

I (kA)	Top	Bottom	Side	Coil	Total	Error (total)
0	0.0%	4.6%	4.6%	0.0%	4.6%	0.9%
5	0.0%	1.5%	1.5%	1.7%	3.2%	0.8%
10	0.2%	1.1%	1.3%	0.5%	1.8%	0.6%
15	0.2%	0.7%	0.9%	2.0%	3.0%	0.7%
20	0.0%	0.9%	0.9%	2.0%	2.9%	0.7%
25	0.0%	0.2%	0.2%	1.3%	1.4%	0.5%
30	0.2%	0.9%	1.1%	1.1%	2.3%	0.6%
35	0.0%	0.2%	0.2%	1.7%	1.8%	0.6%
40	0.4%	0.9%	1.2%	2.3%	3.6%	0.8%

Beam	Fiducial Radius (cm)	Map (15?)	I (kA)	Total # CC events	Top	Bottom	Coil	Exit and Return
he	25	0	0	980	23	180	1	0
he	25	1	5	985	10	85	13	2
he	25	2	10	984	8	61	9	3
he	25	3	15	985	12	68	9	3
he	25	4	20	979	18	62	14	6
he	25	5	25	977	19	61	8	3
he	25	6	30	986	15	58	13	1
he	25	7	35	986	13	61	11	4
he	25	8	40	980	16	42	10	3
he	50	0	0	989	38	190	1	0
he	50	1	5	981	15	98	10	2
he	50	2	10	978	10	75	13	5
he	50	3	15	984	14	76	12	5
he	50	4	20	988	14	65	18	4
he	50	5	25	990	18	86	21	4
he	50	6	30	987	19	71	11	1
he	50	7	35	982	20	70	10	6
he	50	8	40	984	23	73	11	5
le	25	0	0	871	9	84	0	0
le	25	1	5	877	4	48	11	1
le	25	2	10	869	13	33	10	3
le	25	3	15	879	9	37	21	2
le	25	4	20	894	1	38	6	2
le	25	5	25	866	4	25	11	5
le	25	6	30	889	10	35	9	2
le	25	7	35	886	7	21	13	2
le	25	8	40	884	13	32	13	4
le	50	0	0	891	5	95	0	0
le	50	1	5	881	8	68	6	1
le	50	2	10	893	11	43	11	3
le	50	3	15	895	4	37	16	2
le	50	4	20	888	5	37	20	5
le	50	5	25	878	3	37	19	3
le	50	6	30	872	6	49	12	0
le	50	7	35	872	5	47	13	1
le	50	8	40	865	2	35	17	2
me	25	0	0	958	9	107	0	0
me	25	1	5	962	7	47	21	1
me	25	2	10	964	5	37	17	1
me	25	3	15	960	9	34	16	0
me	25	4	20	959	5	20	20	2
me	25	5	25	957	11	35	19	0
me	25	6	30	970	6	39	21	1
me	25	7	35	954	3	37	22	1
me	25	8	40	957	9	28	13	0
me	50	0	0	966	12	101	0	0
me	50	1	5	956	12	68	11	0
me	50	2	10	964	5	52	19	0
me	50	3	15	962	7	41	20	0
me	50	4	20	953	7	50	16	0
me	50	5	25	959	7	53	22	2
me	50	6	30	960	4	52	13	1
me	50	7	35	959	7	43	22	2
me	50	8	40	963	8	44	19	2

Beam	Fiducial	I (kA), he, 25 cm	Top	Bottom	Side	Coil	Total	Error (total)	E&R
he	25	0	2.3%	18.4%	20.7%	0.1%	20.8%	1.3%	0.0%
he	25	5	1.0%	8.6%	9.6%	1.3%	11.0%	1.0%	0.2%
he	25	10	0.8%	6.2%	7.0%	0.9%	7.9%	0.9%	0.3%
he	25	15	1.2%	6.9%	8.1%	0.9%	9.0%	0.9%	0.3%
he	25	20	1.8%	6.3%	8.2%	1.4%	9.6%	0.9%	0.6%
he	25	25	1.9%	6.2%	8.2%	0.8%	9.0%	0.9%	0.3%
he	25	30	1.5%	5.9%	7.4%	1.3%	8.7%	0.9%	0.1%
he	25	35	1.3%	6.2%	7.5%	1.1%	8.6%	0.9%	0.4%
he	25	40	1.6%	4.3%	5.9%	1.0%	6.9%	0.8%	0.3%
		I (kA), he, 50 cm	Top	Bottom	Side	Coil	Total	Error (total)	E&R
he	50	0	3.8%	19.2%	23.1%	0.1%	23.2%	1.3%	0.0%
he	50	5	1.5%	10.0%	11.5%	1.0%	12.5%	1.1%	0.2%
he	50	10	1.0%	7.7%	8.7%	1.3%	10.0%	1.0%	0.5%
he	50	15	1.4%	7.7%	9.1%	1.2%	10.4%	1.0%	0.5%
he	50	20	1.4%	6.6%	8.0%	1.8%	9.8%	0.9%	0.4%
he	50	25	1.8%	8.7%	10.5%	2.1%	12.6%	1.1%	0.4%
he	50	30	1.9%	7.2%	9.1%	1.1%	10.2%	1.0%	0.1%
he	50	35	2.0%	7.1%	9.2%	1.0%	10.2%	1.0%	0.6%
he	50	40	2.3%	7.4%	9.8%	1.1%	10.9%	1.0%	0.5%
		I (kA), le, 25 cm	Top	Bottom	Side	Coil	Total	Error (total)	E&R
le	25	0	1.0%	9.6%	10.7%	0.0%	10.7%	1.0%	0.0%
le	25	5	0.5%	5.5%	5.9%	1.3%	7.2%	0.9%	0.1%
le	25	10	1.5%	3.8%	5.3%	1.2%	6.4%	0.8%	0.3%
le	25	15	1.0%	4.2%	5.2%	2.4%	7.6%	0.9%	0.2%
le	25	20	0.1%	4.3%	4.4%	0.7%	5.0%	0.7%	0.2%
le	25	25	0.5%	2.9%	3.3%	1.3%	4.6%	0.7%	0.6%
le	25	30	1.1%	3.9%	5.1%	1.0%	6.1%	0.8%	0.2%
le	25	35	0.8%	2.4%	3.2%	1.5%	4.6%	0.7%	0.2%
le	25	40	1.5%	3.6%	5.1%	1.5%	6.6%	0.8%	0.5%
		I (kA), le, 50 cm	Top	Bottom	Side	Coil	Total	Error (total)	E&R
le	50	0	0.6%	10.7%	11.2%	0.0%	11.2%	1.1%	0.0%
le	50	5	0.9%	7.7%	8.6%	0.7%	9.3%	1.0%	0.1%
le	50	10	1.2%	4.8%	6.0%	1.2%	7.3%	0.9%	0.3%
le	50	15	0.4%	4.1%	4.6%	1.8%	6.4%	0.8%	0.2%
le	50	20	0.6%	4.2%	4.7%	2.3%	7.0%	0.9%	0.6%
le	50	25	0.3%	4.2%	4.6%	2.2%	6.7%	0.8%	0.3%
le	50	30	0.7%	5.6%	6.3%	1.4%	7.7%	0.9%	0.0%
le	50	35	0.6%	5.4%	6.0%	1.5%	7.5%	0.9%	0.1%
le	50	40	0.2%	4.0%	4.3%	2.0%	6.2%	0.8%	0.2%
		I (kA), me, 25 cm	Top	Bottom	Side	Coil	Total	Error (total)	E&R
me	25	0	0.9%	11.2%	12.1%	0.0%	12.1%	1.1%	0.0%
me	25	5	0.7%	4.9%	5.6%	2.2%	7.8%	0.9%	0.1%
me	25	10	0.5%	3.8%	4.4%	1.8%	6.1%	0.8%	0.1%
me	25	15	0.9%	3.5%	4.5%	1.7%	6.1%	0.8%	0.0%
me	25	20	0.5%	2.1%	2.6%	2.1%	4.7%	0.7%	0.2%
me	25	25	1.1%	3.7%	4.8%	2.0%	6.8%	0.8%	0.0%
me	25	30	0.6%	4.0%	4.6%	2.2%	6.8%	0.8%	0.1%
me	25	35	0.3%	3.9%	4.2%	2.3%	6.5%	0.8%	0.1%
me	25	40	0.9%	2.9%	3.9%	1.4%	5.2%	0.7%	0.0%
		I (kA), me, 50 cm	Top	Bottom	Side	Coil	Total	Error (total)	E&R
me	50	0	1.2%	10.5%	11.7%	0.0%	11.7%	1.0%	0.0%
me	50	5	1.3%	7.1%	8.4%	1.2%	9.5%	0.9%	0.0%
me	50	10	0.5%	5.4%	5.9%	2.0%	7.9%	0.9%	0.0%
me	50	15	0.7%	4.3%	5.0%	2.1%	7.1%	0.8%	0.0%
me	50	20	0.7%	5.2%	6.0%	1.7%	7.7%	0.9%	0.0%
me	50	25	0.7%	5.5%	6.3%	2.3%	8.6%	0.9%	0.2%
me	50	30	0.4%	5.4%	5.8%	1.4%	7.2%	0.8%	0.1%
me	50	35	0.7%	4.5%	5.2%	2.3%	7.5%	0.9%	0.2%
me	50	40	0.8%	4.6%	5.4%	2.0%	7.4%	0.8%	0.2%

ND CC Muon Leakage

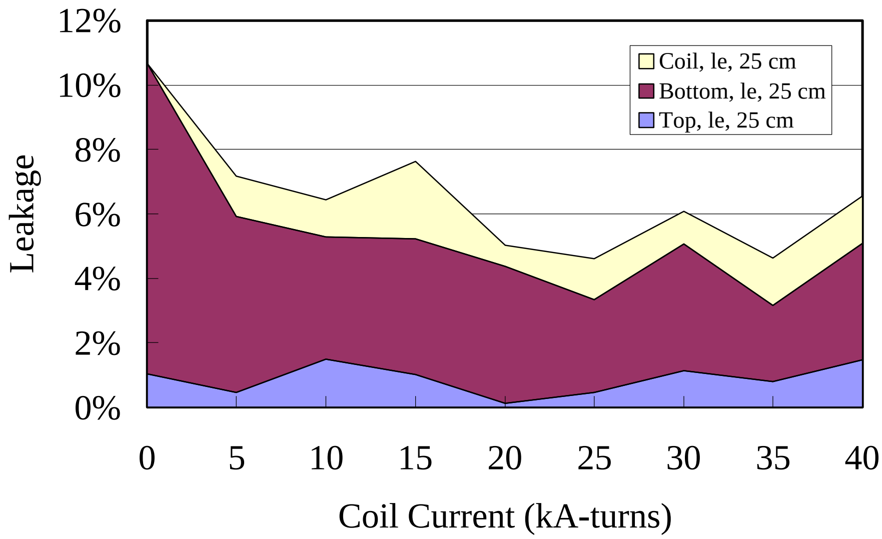

LE (E_ν<8GeV, 25cm Fiducial Region)

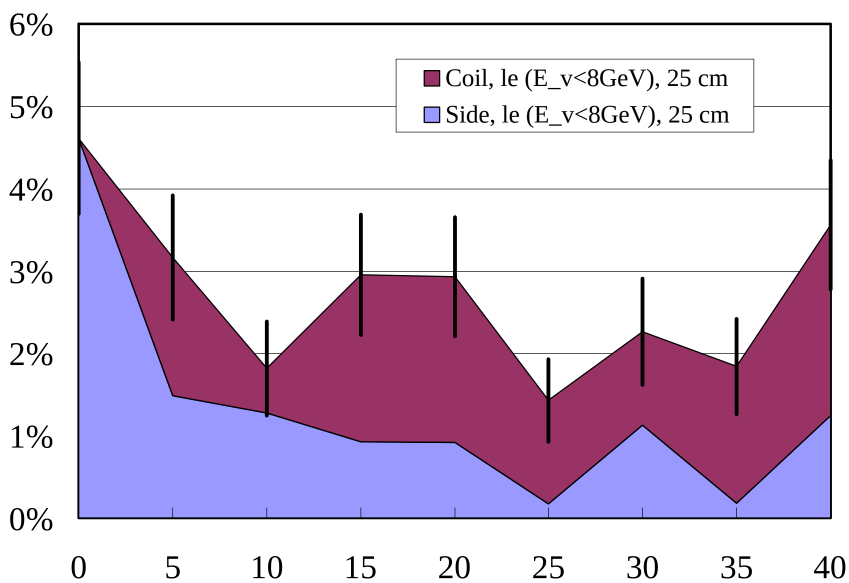

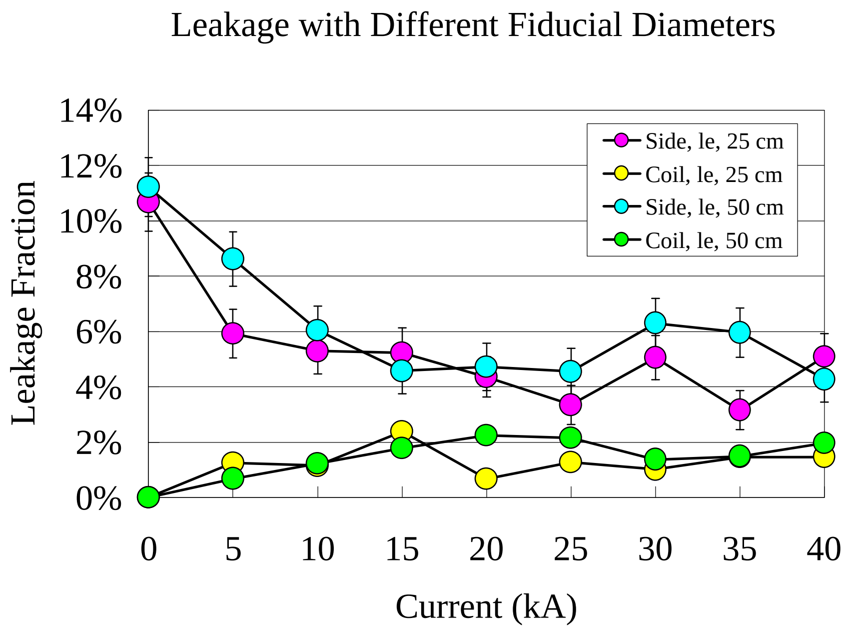

Leakage with Different Fiducial Diameters
Side, le, 25 cm
Coil, le, 25 cm
Side, le, 50 cm
Coil, le, 50 cm
Leakage Fraction
14%
12%
10%
8%
6%
4%
2%
0%
0
5
10
15
20
25
30
35
40
Current (kA)

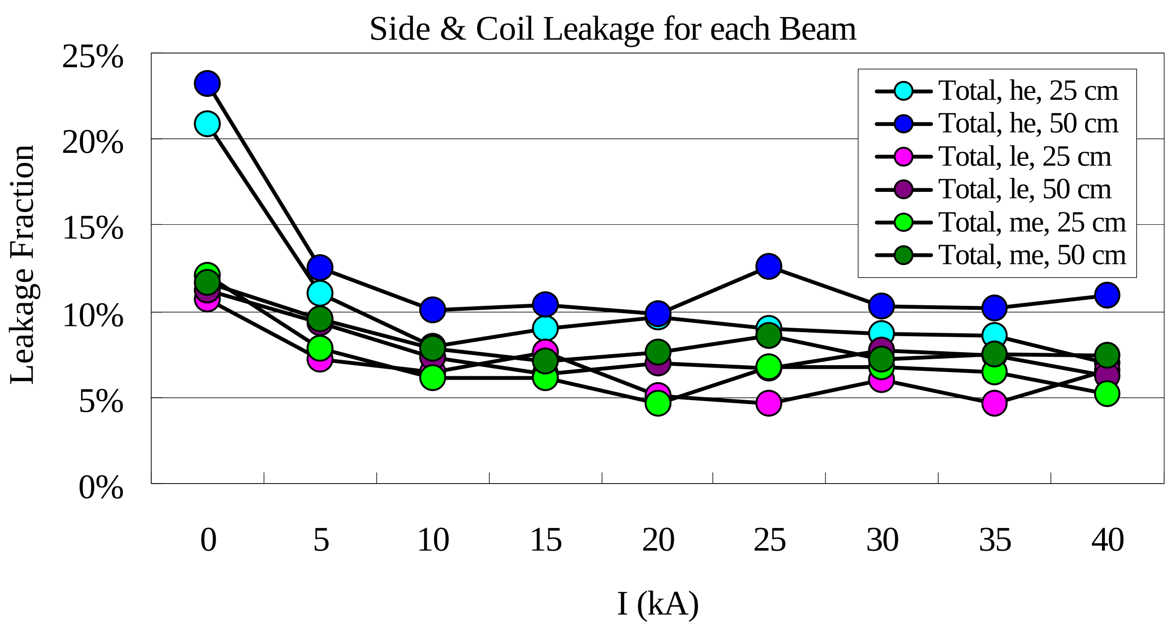

Side & Coil Leakage for each Beam
Total, he, 25 cm
Total, he, 50 cm
Total, le, 25 cm
Total, le, 50 cm
Total, me, 25 cm
Total, me, 50 cm
Leakage Fraction
25%
20%
15%
10%
5%
0%
0
5
10
15
20
25
30
35
40
I (kA)

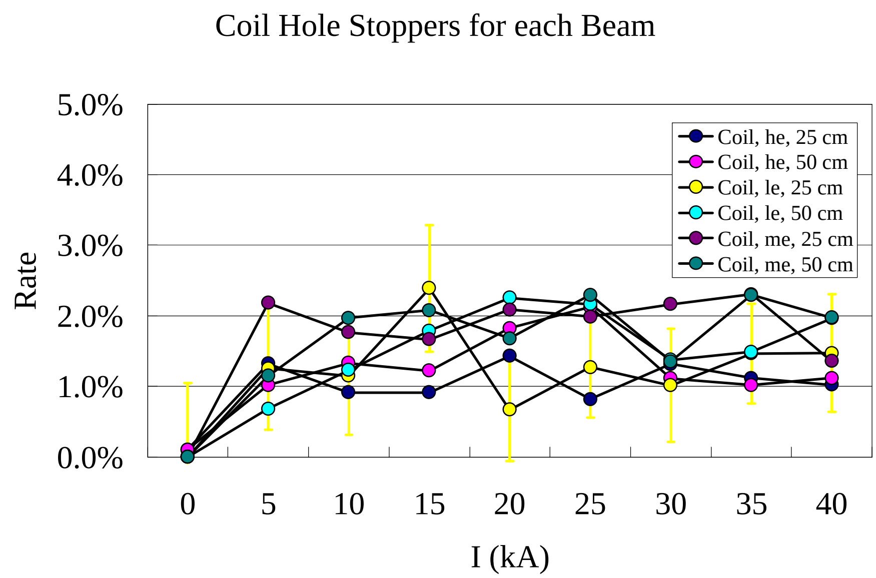

Summary

For any MINOS beams under consideration any ND current above 20kA-turns is acceptable for containment of fiducial CC muons. We also found that coil-stopping muons are not a significant issue in the magnetic design of the detector. Therefore the mean-field specification (and hence magnet's current specification) is not strongly driven by the primary MINOS physics signature (CC energy spectra). Other possible muon samples (e.g. cosmic rays) may provide more stringent requirements. The near/far absolute energy scale calibration requires selection of tracks with a similar range of momenta (and hence dE/dx) in the two detectors.